proceedings

MDPI

Proceedings

Bi2Te3 and Sb2Te3 Thin Films with Enhanced Thermoelectric Properties for Flexible Thermal Sensors †

Eliana Vieira [1,*], Joana Figueira [2], Ana Lucia Pires [3], José Grilo [1], Manuel Fernando Silva [1], André Miguel Pereira [3] and Luís Miguel Goncalves [1]

[1] CMEMS-UMINHO, University of Minho, Campus Azurem, 4804-533 Guimaraes, Portugal; jose_egrl@hotmail.com (J.G.); fsilva@dei.uminho.pt (M.F.S.); lgoncalves@dei.uminho.pt (L.M.G.)

[2] i3N/CENIMAT, Department of Materials Science, Faculty of Science and Technology, Universidade NOVA de Lisboa and CEMOP/UNINOVA, Campus de Caparica 2829, 516 Caparica, Portugal; joanarsfigueira@msn.com

[3] IFIMUP and IN-Institute of Nanoscience and Nanotechnology, Physics and Astronomy Department, Faculty of Science of University of Porto, Rua Campo Alegre, 687, 4769-007 Porto, Portugal; pires.analuci@gmail.com (A.L.P.); ampereira@fc.up.pt (A.M.P.)

* Correspondence: evieira@dei.uminho.pt; Tel.: +351-253-510-190

† Presented at the Eurosensors 2018 Conference, Graz, Austria, 9–12 September 2018.

Published: 11 December 2018

Abstract: The influence of substrate type in boosting thermoelectric properties of co-evaporated Bi2Te3 and Sb2Te3 films (with 400 nm-thick) is here reported. Optimized power factor values are 2.7×10^{-3} W K^{-2} m^{-1} and 1.4×10^{-3} W K^{-2} m^{-1} for flexible Bi2Te3 and Sb2Te3 films, respectively. This is an important result as it is at least 2 times higher than the power factor found in the literature for flexible Bi2Te3 and Sb2Te3 films. A flexible infrared thermopile sensor was developed with high detectivity (2.50×10^{7} cm $\sqrt{\text{Hz}}$W^{-1}).

Keywords: telluride alloys; flexible materials; thermoelectricity; IR sensor device

1. Introduction

Thermoelectric (TE) technology appears as a green energy source due to their direct transformation of small thermal gradients into electric power, and vice-versa, in a renewable manner and without CO_2 emissions. Telluride alloys have attracted a great deal of interest because of their potential applications as TE generators, TE coolers and thermal sensors [1,2]. The performance of TE devices is highly dependent on TE properties of constituent materials, namely the Seebeck coefficient (S), the electrical conductivity(σ) and the thermal conductivity (k), according to the figure of merit (ZT), $ZT = S^2\sigma/k$, where $S^2\sigma$ is related to the power factor, PF. High TE device performance require high ZT and PF values. To get high sensitive thermal sensors, TE materials with high S values are required. Thin films instead of conventional *bulk* materials opens the possibility to reduce substantially the material amount required, and enable the deposition on flexible substrates, making the devices compatible with modern integrated circuit technology.

A pioneering work that reports the effect of both substrate thickness and type on the TE properties of Sb_2Te_3 and Bi_2Te_3 films, is here discussed. A simple and flexible p-n TE device have been fabricated and tested for pyrometry applications.

2. Material and Methods

Sb_2Te_3 and Bi_2Te_3 films (with 400 nm-thick) were fabricated by co-evaporation method in a high-vacuum chamber (10^{-6} mbar). Bi (or Sb) evaporation rate was 2 Å/s and Te evaporation rate was 6 Å/s. Borosilicate glass and Kapton® substrates (with 50- and 25 μm—thick) were used for films deposition. Substrates were heated at 270 °C and 230 °C, for the deposition of Sb_2Te_3 and Bi_2Te_3 films, respectively. The morphology and chemical composition of the films were obtained by scanning electron microscopy (SEM) and Energy-Dispersive X-ray spectroscopy (EDX). The crystallographic structure was obtained by X-ray diffraction (XRD). In-plane electrical conductivity was measured at room temperature (RT) using the conventional 4-Probe van der Pauw geometry. Seebeck coefficients were obtained by connecting one side of the film to a heated metal block at a fixed temperature and the other side to a heatsink at room temperature, to have a temperature gradient (of a few kelvin) along the film. A flexible thermopile infrared (IR) detector based on the p-n junction (5 × 5 mm^2), with a conductive carbon paint as absorber, was developed. The radiation was emitted by a black body target object (15 cm diameter) from 293 K to 513 K of temperature and at a distance of 3 cm. The thermo-voltage generated by the device was monitored by a multimeter.

3. Results and Discussion

The thermoelectric voltage generated by the telluride alloys shows a linear dependence of temperature gradient (Figure 1a,b). Maximum S values of—224 μV K^{-1} (for Sb_2Te_3 film) and 184 μV K^{-1} (for Sb_2Te_3 film) deposited on 25 μm—thick Kapton® substrates were obtained, respectively. The negative (positive) slope for Sb_2Te_3 (Sb_2Te_3) films is consistent with n-type (p-type) semiconductor behavior. The surface morphology and chemical composition of the films deposited on the three substrates are also shown on Figure 1.

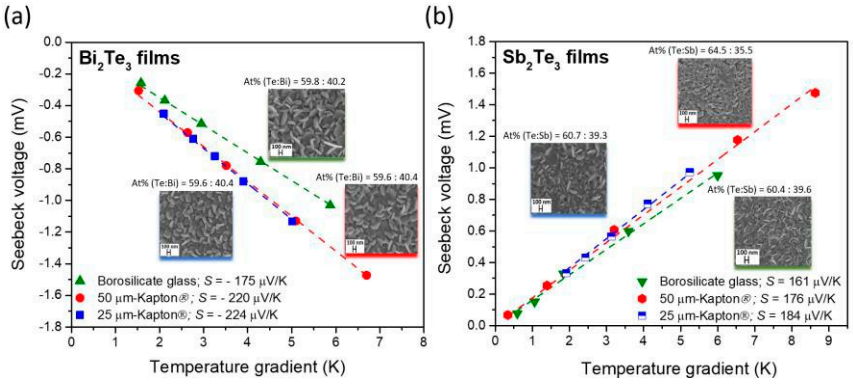

Figure 1. Seebeck voltage measured as a function of the induced temperature gradient for (**a**) Bi_2Te_3 and (**b**) Sb_2Te_3 films deposited on the three substrates. S values calculated from the slope are included. Surface morphology of all films are shown, with corresponding chemical composition of the alloy.

Stoichiometric Bi_2Te_3 films (At%(Te/Bi) ≈ 1.5) show a dense and grain morphology with large flakes (Figure 1a). However, the film deposited on 25 μm—Kapton® shows a more compact structure with more rounded domains. Sb_2Te_3 films show a similar surface morphology except for the film deposited on 50 μm—thick Kapton® that appears more flat and dense, with smaller crystals. While the films deposited on Kapton® substrates are stoichiometric Sb_2Te_3, the film deposited on glass shows a At%(Te) higher than the others films (~1.8). Highest σ values are obtained for Bi_2Te_3film deposited on 25 μm—Kapton® (≈5.3 × 10^4 $(\Omega\ m)^{-1}$) and for the Bi_2Te_3 film deposited on 50 μm—Kapton® (≈ 4.6 × 10^4 $(\Omega\ m)^{-1}$), resulting in the highest PF values of 2.7 × 10^{-3} W K^{-2} m^{-1} (Bi_2Te_3) and 1.4 × 10^{-3} W K^{-2} m^{-1} (Sb_2Te_3) (Table 1). σ values of Bi_2Te_3 films deposited on glass and 50 μm—thick Kapton® substrates are 1.2 × 10^4 $(\Omega\ m)^{-1}$ and 2.8 × 10^4 $(\Omega\ m)^{-1}$, respectively. For Sb2Te3 films, σ values of 3.0 × 10^4 $(\Omega\ m)^{-1}$ (for glass) and 3.2 × 10^4 $(\Omega\ m)^{-1}$ (for 25 μm - Kapton®) are obtained. The films with highest PF values revealed a more compact and dense structure (so, more connected grains). Disoriented grains create a higher electrical resistivity due to a more open structure. XRD spectrum of the Bi_2Te_3 film with the

highest *PF* value (Figure 2a) shows a preferential growth along the (0 0 15) plane of the Bi_2Te_3 crystals. Similar XRD patterns of Sb_2Te_3 films (Figure 2b) are observed.

A flexible infrared thermopile sensor based on a single p-n junction has been tested as a proof of concept. The 25 μm Kapton® provides flexibility and lightness to the devices, while it offers high upper working temperature (until 350 °C) and low thermal conductivity (0.12 W m^{-1} K^{-1}). A metal structure was constructed to maintain the cold junctions at RT (heat sink) and to allow only the region of the hot junction to receive the radiation (through a hole in the metal structure), as shown in the Figure 3a.

Table 1. Comparison of TE properties of the Bi_2Te_3 and Sb_2Te_3 in the present study with other reported by other authors (with different techniques).

Film	Thickness (μm)	Substrate	S (μVK^{-1})	σRT (Ω m)$^{-1}$	PF(× 10^{-3} W K^{-2} m^{-1})
Bi_2Te_3/Sb_2Te_3	0.4	glass/polyimide	−224/176	$5.3 \times 10^4/4.6 \times 10^4$	2.7/1.4
Sb_2Te_3 [3]	-	polyimide	135	2.8×10^4	0.5
Bi_2Te_3 [4]	1.3	polyimide	119	7.0×10^4	1 (Bi2Te3)
$Sb_2Te_3/Bi_{1.8}Te_{3.2}$ [5]	70	Glass-textile/polyimide	−138/120	$1.0 \times 10^4/1.0 \times 10^4$	0.3/0.2

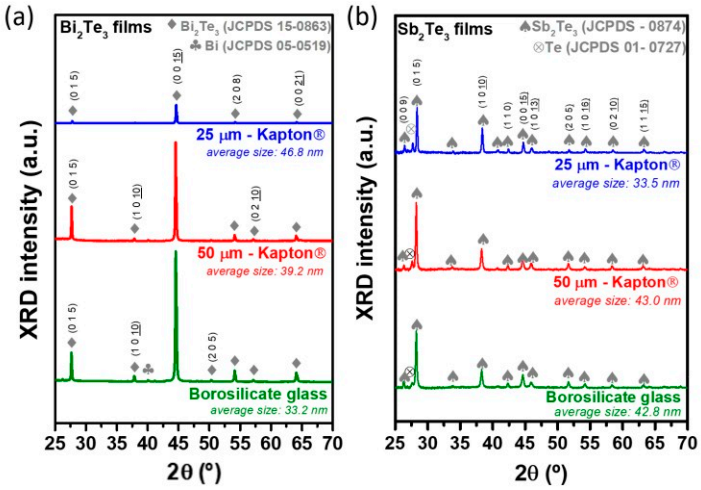

Figure 2. XRD patterns for (**a**) Bi_2Te_3 and (**b**) Sb_2Te_3 films deposited on the three substrates. Average NCs size is indicated for each film. The presence of Bi (for Bi_2Te_3 films) and Te (for Sb_2Te_3 films) diffraction peaks confirms that the films are Bi- and Te-rich.

An example of the thermal test is given in the Figure 3b. Figure 3c shows that the experimental data are fitted with a 4-order polynomial, according to the Equation [6] shown in the inset of Figure 3c. K_s is the instrument factor of the sensor ($K_s = 5.50 \times 10^{-14}$), ε_{targ} is the emissivity of the target disk ($\varepsilon_{targ} = 0.9$), T_{targ} is the temperature of the disk and T_{sens} is the temperature of the sensor. $\varepsilon_{sens} = 1$ considering the internal reflections inside the thermopile case, and therefore, the whole structure behaves as a cavity blackbody with high emissivity [6]. The responsivity (R_s) *is* obtained by the slope of the output voltage as a function of absorbed heat radiation power [2], and is 0.19 V W^{-1} for our sensor. Specific detectivity (D*) can be calculated by [2]

$$D^* = \frac{\sqrt{A_{abs}}\sqrt{\Delta f}}{NEP} \quad (1)$$

where A is area of sensor (25 mm^2) and NEP is the noise equivalent power which is the quotient of RMS of the voltage (v_n) and R_s [2]. A $v_n = 3.9$ nV was obtained taking in account the $\Delta f = 1$ Hz, $T = 298$ K and $R = 910$ Ω. NEP value was estimated to be 20 nW. A D^* value of 2.50×10^7 cm √Hz W^{-1} was obtained.

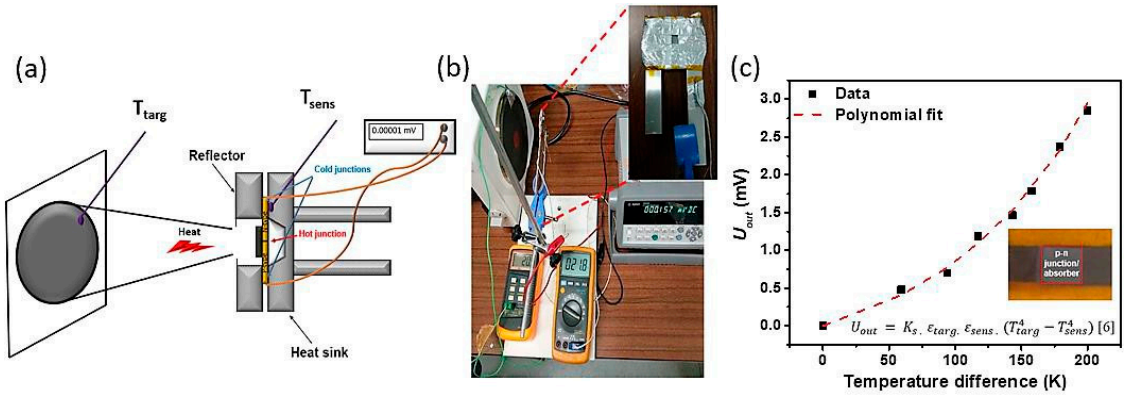

Figure 3. (**a**) Scheme of operation of the TE device used as radiation sensor; (**b**) thermal test (**c**) output voltage plotted against the temperature difference (T_{targ} − T_{sens}); inset: photograph of the sensor and equation [6].

4. Conclusions

The developed telluride films have the highest *PF* values among the results regarding flexible films with thickness below 1 μm, reported up to now. Their high *S* values, together with a flexible structure make them suitable to be applied as flexible thermal sensors, as proven here.

Author Contributions: L.M.G. conceived and designed the experiments; E.V. performed the experiments; E.V., J.F., A.L.P., J.G. analyzed the data; M.F.S. and A.M.P. contributed reagents/materials/analysis tools; E.V. wrote the paper and all authors reviewed the paper.

Acknowledgments: This work is supported by FCT with the reference project UID/EEA/04436/2013, by FEDER funds through the COMPETE 2020—Programa Operacional Competitividade e Internacionalização (POCI) with the reference project POCI-01-0145-FEDER-006941. EMFV and JF is grateful for financial support through the FCT grants SFRH/BPD/95905/2013 and SFRH/BD/121679/2016.

Conflicts of Interest: The authors declare no conflict of interest. The founding sponsors had no role in the design of the study; in the collection, analyses, or interpretation of data; in the writing of the manuscript, and in the decision to publish the results.

References

1. Mamur, H.; Bhuiyan, M.R.A.; Korkmaz, F.; Nil, M. A review on bismuth telluride (Bi_2Te_3) nanostructure for thermoelectric applications. *Renew. Sustain. Energy Rev.* **2018**, *82*, 4159–4169. doi:10.1016/j.rser.2017.10.112.
2. Xu, D.; Xiong, B.; Wang, Y. Micromachined thermoelectric IR sensors fabricated by a self-aligned process. *Smart. Mater. Struct.* **2011**, *20*, 015013-21. doi:10.1088/0964-1726/20/1/015013.
3. Shen, S.; Zhu, W.; Deng, Y.; Zhao, H.; Peng, Y.; Wang, C. Enhancing thermoelectric properties of Sb_2Te_3 flexible thin film through microstructure control and crystal preferential orientation engineering. *Appl. Surf. Sci.* **2017**, *414*, 197–204. doi:10.1016/j.apsusc.2017.04.074.
4. Nuthongkum, P.; Sakdanuphab, R.; Horprathum, M.; Sakulkalavek, A. [Bi]:[Te] Control, Structural and Thermoelectric Properties of Flexible BixTey Thin Films Prepared by RF Magnetron Sputtering at Different Sputtering Pressures. *J. Electron. Mater.* **2017**, *46*, 6444–6450. doi:10.1007/s11664-017-5671-x.
5. Cao, Z.; Tudor, M.J.; Torah, R.N.; Beeby, S.P. Screen Printable Flexible BiTe–SbTe-Based Composite Thermoelectric Materials on Textiles for Wearable Applications. *IEEE Trans. Electron. Devices* **2016,** *63,* 4024–4030. doi:10.1109/TED.2016.2603071.
6. Sebastián, E.; Armiens, C.; Gómez-Elvira, J. Infrared temperature measurement uncertainty for unchopped thermopile in presence of case thermal gradients. *Infrared Phys. Technol.* **2011**, *54*, 75–83. doi:10.1016/j.infrared.2010.12.038.